ISOTHERMAL AND NON-ISOTHERMAL OSCILLATIONS OF A PSEUDOELASTIC OSCILLATOR: LYAPUNOV EXPONENTS ESTIMATION

Luciano G. Machado, luciano@tamu.edu
Dimitris C. Lagoudas, lagoudas@tamu.edu
Texas A & M University, Department of Aerospace Engineering.
College Station, TX, 77843-3141, USA

Marcelo A. Savi, savi@mecanica.ufrj.br
Universidade Federal do Rio de Janeiro, COPPE - Department of Mechanical Engineering.
P.O. Box 68.503, 21941-972, Rio de Janeiro, RJ, Brazil

Abstract. *Shape memory alloys (SMAs) have been used in different kind of application including those that explore their dynamical response. The key characteristics of SMAs are associated with adaptive dissipation related to their hysteretic behavior and changes in their material properties caused by martensitic phase transformations. This work discusses the dynamical response of one-degree of freedom (1-DOF) oscillator where the restitution force is provided by an SMA pseudoelastic element described by a smooth constitutive model built upon the Boyd-Lagoudas model. The case of non-isothermal heat transfer conditions is here investigated and then compared to the isothermal case. Numerical simulations shows a very intricate dynamic response of the system, with even chaotic responses. Phase Space curves, Poincaré Maps and Lyapunov exponents are used to determine the nature of the motion of the system, in both isothermal and non-isothermal cases.*

Keywords: *Shape memory alloy (SMA), Lyapunov exponents, Nonlinear dynamics, chaos, Thermomechanical coupling.*

1. INTRODUCTION

Shape memory alloys (SMAs) have been used in different applications and their highly nonlinear characteristics can promote a very intricate dynamic behavior. Several applications in different field of engineering are exploring SMAs' dynamical response, being associated with both adaptive dissipation related to their hysteretic behavior, and changes in their material properties caused by martensitic phase transformation.

The hysteretic behavior of pseudoelastic SMAs provides them high energy damping capacity, while the phase transformation changes the thermomechanical properties. Hysteretic damping can be used to attenuate undesired vibrations of a mechanical system or structure, while variable stiffness can alter the resonance frequency and vibration isolation frequency of the system. Several references, such as Williams *et al.* (2002), Salich *et al.* (2001), Saadat *et al.* (2002), and Oberaigner *et al.* (2002), have investigated the use of SMA braces and cables in structures, for the purpose of vibration isolation and damping control.

The intrinsic energy dissipation (damping) characteristics of SMAs is a very complex phenomenon and can be a function of several factors, such as loading history of the material, temperature, amplitude and frequency of the response, strain loading/unloading rates, and heat transfer of the surrounding medium. Since latent heat can be generated/absorbed during stress-induced martensitic phase transformations, temperature variations can occur on the material, altering its pseudoelastic response. Therefore, the thermomechanical coupling is a key factor to be considered. Several references have experimentally investigated the effect of strain rates and the heat transfer of the medium in the pseudoelastic response of SMAs, such as Leo *etal.* (1993), Shaw and Kyriakides (1995), and others.

Even though the evolving thermomechanical properties and high damping capacity are very interesting characteristics to be explored in passive vibration isolation and damping systems, they can also lead to a very complex dynamic response. SMAs systems can present a very rich class of responses, where even chaotic behavior can take place. Therefore, it is of fundamental importance to study the nonlinear dynamic response of SMA systems, especially in non-isothermal heat transfer conditions, if one wants to use them in vibration isolation control systems. Several references have investigated numerically the complex dynamic response of SMA systems, including the possibility of chaotic responses, such as in Feng and Li (1996), Savi and Pacheco (2002), Machado *et al.* (2003), Lacarbonara and Vestroni (2003), Lagoudas *et al.* (2004), Machado and Lagoudas (2004), Bernardini and Rega (2005), and Savi *et al.* (2006).

This work discusses the dynamical response of SMA system considering a 1-DOF oscillator, where the restitution force is provided by a pseudoelastic SMA element. A thermomechanical constitutive model built upon the constitutive model introduced by Boyd and Lagoudas (1996) is used to simulate the SMA constitutive behavior. The model is developed under the same thermomechanical framework introduced by Boyd and Lagoudas (1996);but with a new hardening function. This new hardening function guarantees smooth transitions between elastic and transformation regimes. Since

SMAs exhibit a strong thermomechanical coupling, caused by the presence of latent heat during phase transformation, the heat equation is introduced into the constitutive formulation, so that the effect of temperature variations caused by phase transformation can also be predicted. The introduction of the heat equation also leads to a time-dependent behavior of the SMA device even though the constitutive model is rate-independent. Numerical simulations of the oscillator are conducted for the cases forced vibrations in both isothermal and non-isothermal conditions, with special attention to the chaotic vibrations. Phase space plots and Lyapunov exponents are the tools used to classify the motion of the oscillator. Lyapunov exponents are estimated by employing the classical algorithm by Wolf *et al.* (1985) adopting a proper linearization of the system.

2. 1-DOF SMA PSEUDOELASTIC OSCILLATOR

The SMA system analyzed in this article is a single-degree of freedom oscillator (Fig. 1), which consists of a mass m attached to a SMA element of length L and cross-section area A. The system is harmonically excited by a force $f(t) = F_0 \sin(2\pi f t)$.

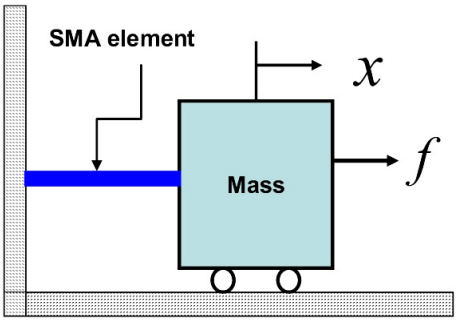

Figure 1. 1-DOF SMA Pseudoelastic Oscillator

The equation of motion of the oscillator is given by

$$m\ddot{x} + F_{SMA} = F_0 \sin(2\pi f t) \tag{1}$$

where x is the mass displacement, f is the forcing frequency, F_0 is the amplitude of exciting force, F_{SMA} is the force exerted by the SMA element.

An important observation is that since the SMA is rate independent, the dissipation in the system is due to hysteresis only, which is path dependent. As a consequence, no velocity dependent term due to rate dependent dissipation, such as in viscoelastic materials, appears in Eq. 1. The time dependence will be later introduced by considering the thermomechanical coupling into the formulation of the constitutive model for SMAs.

Next session presents the constitutive model used to describe the SMA behavior. Since the model works with stress σ, and strain ε, and Eq. 1 is described as a function of forces and displacements, one can correlate stress with forces and displacement with strains through the following relations: $F_{SMA} = \sigma \cdot A$ and $\varepsilon = x/L$. In all the numerical simulations the mass was considered to be $m = 1kg$, and the area and length of the SMA element were $A = 2.0 \cdot 10^{-7} m^2$, and $L = 0.08m$, respectively.

2.1 Smooth Constitutive Model for SMAs

This section presents the constitutive model used in this work to simulate the SMA behavior. The model is developed under the same thermomechanical framework proposed by Boyd and Lagoudas (1996). The main difference between the model by Boyd and Lagoudas (1996) and the model presented here is the hardening function utilized to describe the transformation hardening behavior of SMAs, which allows smooth transitions between elastic and transformation regimes.

Originally, the constitutive model proposed by Boyd and Lagoudas (1996) was formulated using a free energy function and dissipation potentials as in rate-independent plasticity, where for a given strain and temperature loading/unloading path input, stress output is provided. The constitutive model considers a total specific Gibbs free energy, G, of a polycrystalline SMA, as a function of the independent state variables: stress $\boldsymbol{\sigma}$, and temperature T, and also of the internal state variables: martensitic volume fraction ξ, and transformation strain $\boldsymbol{\varepsilon}^t$. In this formulation the martensitic volume fraction is assumed to be a scalar quantity, and it includes the volume fractions of all martensitic variants present in the material. The total Gibbs free energy (Qidwai and Lagoudas, 2000) is then proposed as:

$$G\left(\boldsymbol{\sigma}, T, \xi, \boldsymbol{\varepsilon}^t\right) = -\frac{1}{2\rho}\boldsymbol{\sigma} : \mathcal{S} : \boldsymbol{\sigma} - \frac{1}{\rho}\boldsymbol{\sigma} : \left[\boldsymbol{\alpha}\left(T - T_0\right) + \boldsymbol{\varepsilon}^t\right] + C\left[\left(T - T_0\right) - T\ln\left(\frac{T}{T_0}\right)\right] - s_0 T + u_0 + f(\xi) \tag{2}$$

where T_0 is the reference state temperature. The material constants $\mathcal{S}$,$\boldsymbol{\alpha}$,ρ ,C ,s_0 ,u_0 are the effective compliance tensor, effective thermal expansion coefficient, density, effective specific heat, effective specific entropy at the reference state, and the effective specific internal energy at the reference state, respectively. The form of the hardening function, $f(\xi)$, will be presented later. The effective material properties can be defined in terms of the martensitic volume fraction, ξ, by the rule of mixtures, as $(\cdot) = (\cdot)^A + \xi\left[(\cdot)^M - (\cdot)^A\right]$, where the superscript A stands for austenitic phase, while the superscript M stands for the martensitic phase.

Constitutive relations are obtained by following a standard thermodynamic procedure, where the Gibbs free energy and the internal energy, which are related through the Legendre transformation (Table. 1), are substituted into the first law and second law of thermodynamics as expressed in the Clausius-Duhem inequality (Coleman and Gurtin, 1967). The total infinitesimal strain tensor and entropy are derived as follows:

$$\varepsilon = -\rho\frac{\partial G}{\partial \boldsymbol{\sigma}} = \mathcal{S} : \boldsymbol{\sigma} + \boldsymbol{\alpha}\left(T - T_0\right) + \boldsymbol{\varepsilon}^t \tag{3}$$

$$s = -\frac{\partial G}{\partial T} = \boldsymbol{\sigma} : \boldsymbol{\alpha} + C\ln\left(\frac{T}{T_0}\right) + s_0 \tag{4}$$

Table 1 presents a summary of the equations of Boyd and Lagoudas (1996) model.

Table 1. Summary of the Boyd and Lagoudas model equations for polycrystalline SMAs.

Legendre Transformation:

$u = G + Ts + \frac{1}{\rho}\boldsymbol{\sigma} : \boldsymbol{\varepsilon}$

Evolution Equation of the Transformation Strain (Flow Rule):

$\dot{\boldsymbol{\varepsilon}}^t = \boldsymbol{\Lambda}\dot{\xi}$, where $\boldsymbol{\Lambda}$ is the transformation tensor

Dissipation Inequality:

$\left(\boldsymbol{\sigma} : \boldsymbol{\Lambda} - \rho\frac{\partial G}{\partial \xi}\right)\dot{\xi} = \pi\dot{\xi} \geq 0$

Thermodynamic Force (π) Conjugated to ξ:

$\pi = \boldsymbol{\sigma} : \boldsymbol{\Lambda} + \frac{1}{2}\boldsymbol{\sigma} : \Delta\mathcal{S} : \boldsymbol{\sigma} + \boldsymbol{\sigma} : \Delta\boldsymbol{\alpha}\left(T - T_0\right) + \rho\Delta C\left[\left(T - T_0\right) - T\ln\left(\frac{T}{T_0}\right)\right] + \rho\Delta s_0 T + \rho\Delta u_0 - \frac{\partial f(\xi)}{\partial \xi}$

Transformation Function Φ:

$\Phi = \pi - Y^*; \quad \dot{\xi} > 0 \qquad$ or $\qquad \Phi = -\pi - Y^*; \quad \dot{\xi} < 0$

where Y^* is a measure of dissipation due to microstructural arrangements.

Kuhn-Tucker Conditions:

$\dot{\xi} > 0 \quad$ or $\quad \dot{\xi} < 0\,; \qquad \Phi\left(\sigma, T, \xi\right) \leq 0; \qquad \Phi\dot{\xi} = 0$

Consistency Condition:

$\dot{\Phi} = 0$

The transformation function Φ and the Kuhn-Tucker conditions (Tab. 1) are utilize to define the elastic regime and conditions for the onset of phase transformation (Boyd and Lagoudas, 1996, and Qidwai and Lagoudas, 2000). Whenever the transformation function π reaches the threshold value of Y, or in other words, whenever $\Phi = 0$, the martensitic phase transformation takes place. Moreover, the rate-independent formulation assumes that π is constant during phase transformation (Boyd and Lagoudas, 1996), and that the consistency condition (as in classical plasticity) can be written as $\dot{\Phi} = 0$.

The hardening function $f(\xi)$ is used to describe the interaction between the austenitic and martensitic phases and martensitic variant themselves. The new hardening function proposed in this work is a general polynomial hardening

function, which allows a smooth transition between the elastic and transformation regimes. The new hardening function is not only a continuous function, but also has continuous derivatives. This way, the experimental results can be better described, specially polycrystalline trained SMA wires that shows smooth transition between elastic and transformation regimes (Lagoudas *et al.*, 2005, and Machado and Lagoudas, 2006). The new hardening function is of the form:

$$f(\xi) = \begin{cases} \frac{1}{2}a_1 \left(\xi + \frac{\xi^{n_1+1}}{(n_1+1)} + \frac{(1-\xi)^{n_2+1}}{(n_2+1)} \right) & ; \qquad \dot{\xi} > 0 \\ \frac{1}{2}a_2 \left(\xi + \frac{\xi^{n_3+1}}{(n_3+1)} + \frac{(1-\xi)^{n_4+1}}{(n_4+1)} \right) & ; \qquad \dot{\xi} < 0 \end{cases} \tag{5}$$

where a_1 and a_2 are model parameters that are defined as functions of the material parameters. n_1, n_2, n_3 and n_4 are the polynomial exponents that can assume values as either integers or rational numbers.

It is important to mention that the cases of isothermal and adiabatic heat transfer conditions are still rate independent, but extreme cases. Therefore, heat transfer cases that are neither isothermal nor adiabatic can be modeled by including the heat equation into the constitutive model. The fully thermomechanical coupled heat equation can be derived, by combining the total strain (Eq. 3), the entropy (Eq. 4) and the first law of thermodynamics, with the time derivative of Eq. 4, where the dissipation inequality (Table 1) should not be violated at anytime. Therefore, after some manipulation, the three-dimensional form of the heat equation is given as follows:

$$T\boldsymbol{\alpha} : \dot{\boldsymbol{\sigma}} + \rho c\dot{T} + \left(T\boldsymbol{\sigma} : \Delta\boldsymbol{\alpha} - \rho\Delta c T \ln\frac{T}{T_0} + \rho\Delta s_0 T \right) \dot{\xi} = -\nabla \cdot \mathbf{q} + \rho r \tag{6}$$

where the first term on the left-hand side, which is related to the thermoelastic coupling, expresses how the temperature changes due to a variation of the stress level. The second term is related to the thermal energy, while the third term of the left-hand side expresses how the temperature of the SMA changes due to phase transformation. The first and second terms of the right-hand side are related to the heat transfer conditions, where the cases of convection, conduction or resistive heating can be considered depending on the choice of the heat flux vector $\mathbf{q}$, and the internal heat source ρr.

2.2 One-dimensional reduction of the model

Since the SMA element of the oscillator is considered here to be one-dimensional, it is important to reduced the model from its three dimensional form to a one-dimensional one. The thermomechanical constitutive model for SMAs can be reduced for the one-dimensional case by assuming a uniaxial loading of an SMA wire in the x_1-direction. The stress tensor has only one non-zero component, that is

$$\sigma_{11} = \sigma \neq 0 \tag{7}$$

where σ is the applied uniaxial stress.

The transformation strain components are given by

$$\varepsilon^t_{11} = \varepsilon^t; \quad \varepsilon^t_{22} = \varepsilon^t_{33} = -\frac{1}{2}\varepsilon^t; \quad \varepsilon_{ij} = 0; \qquad \mathrm{i,j} = 1, ..., 3 \tag{8}$$

where ε^t is the uniaxial transformation strain assuming that it results in isochoric deformations.

The double dot product between two 2^{nd} order tensors and between a 2^{nd} order tensor and a 4^{th} order tensor, as well as the dot product between two vectors that appear in Eq. 2, Eq. 3,Eq. 4, in Tab. 1, and in Eq. 6 can be reduced to a simple scalar multiplication in the one-dimensional case, where the scalars are the 11- (or 1111-) components of the 2^{nd} (4^{th}) order tensors, and 1-component of the vectors. For the sake of simplicity, the scalar components will be written without indices. For example, σ_{11} will be written as σ and $\mathcal{S}_{1111}$ as S, without boldface. It is also important to mention that the component Λ_{11} is defined as $H\mathrm{sgn}(\sigma)$, where H is the maximum transformation strain for the one-dimensional case and $\mathrm{sgn}(\sigma)$ gives the direction of the transformation for the cases of tensile or compressive loadings.

The evolution equation of the transformation strain becomes

$$\dot{\varepsilon^t} = H\mathrm{sgn}(\sigma)\dot{\xi} \tag{9}$$

The 1D form of the total strain and the entropy are given by

$$\varepsilon = S\sigma + \alpha(T - T_0) + \varepsilon^t \tag{10}$$

Now some assumptions related to the heat transfer on the boundary of the SMA element need to be made. The first assumption is that there is no heat flux leaving or entering the SMA element through their ends. Moreover, radial heat conduction is disregarded since the SMA element are of small diameters. Therefore, no gradient of temperature is

assumed inside the material. As a result, the first term of the right-hand side of Eq. 6 is dropped, and the only heat transfer considered is due to convection. The heat convection is then considered in this formulation as part of the heat input supply, and it is described by Newton's law of cooling given by Eq. 11. Also, other forms of heat transfer could be added in the heat input supply, such as resistive heating, for example.

$$\rho r = h\left(T - T_\infty\right) \tag{11}$$

where h is the heat convection coefficient, T_∞ is the surrounding environment temperature.

The heat equation (Eq. 6) can also be written in a one-dimensional form. Moreover, assuming no temperature gradient throughout the SMA element, one can have

$$T\alpha\dot{\sigma} + \rho c\dot{T} + \left(T\sigma\Delta\alpha - \rho\Delta cT\ln\frac{T}{T_0} + \rho\Delta s_0 T\right)\dot{\xi} = h\left(T - T_\infty\right) \tag{12}$$

2.3 Material Parameters, Model Calibration and Numerical Implementation

At this point it is necessary to define the SMA parameters in order to calibrate the model. The material parameters that will be used throughout the numerical simulation is given by Tab. 2.

Table 2. Material Constants

$E^A = 28.0 \cdot 10^9 Pa$	$E^M = 21.0 \cdot 10^9 Pa$
$\alpha^A = 22.0 \cdot 10^{-6}\mathrm{K}$	$\alpha^M = 22.0 \cdot 10^{-6}\mathrm{K}$
$C^A = 400$	$C^M = 400$
$H = 0.03$	
$T_0 = 293\mathrm{K}$	$\rho\Delta s_0 = -15 \cdot 10^4$
$M^{0f} = 213\mathrm{K}$	$M^{0s} = 269\mathrm{K}$
$A^{0s} = 233\mathrm{K}$	$A^{0f} = 293\mathrm{K}$

The model parameters can be defined as a function of the material parameters presented in Tab. 2, such as, transformation temperatures and the entropy difference per unit volume between the phases. Table 3 presents the expressions describing these model parameters.

Table 3. Model Parameters

$$Y = \tfrac{1}{2}\rho\Delta s_0\left(M_{0s} - A_{0s}\right) + \tfrac{1}{2}\rho\Delta C\left[M_{0s}\left(1 - \ln\left(\tfrac{M_{0s}}{T_0}\right)\right) - A_{0f}\left(1 - \ln\left(\tfrac{A_0 f}{T_0}\right)\right)\right]$$

$$a_1 = \tfrac{1}{2}\rho\Delta s_0\left(M_{0f} - M_{0s}\right) + \tfrac{1}{2}\rho\Delta C\left[M_{0f}\left(1 - \ln\left(\tfrac{M_{0f}}{T_0}\right)\right) - M_{0s}\left(1 - \ln\left(\tfrac{M_0 s}{T_0}\right)\right)\right]$$

$$a_2 = \tfrac{1}{2}\rho\Delta s_0\left(A_{0s} - A_{0f}\right) + \tfrac{1}{2}\rho\Delta C\left[A_{0s}\left(1 - \ln\left(\tfrac{A_{0s}}{T_0}\right)\right) - A_{0f}\left(1 - \ln\left(\tfrac{A_0 f}{T_0}\right)\right)\right]$$

$$\rho\Delta u_0 = \tfrac{1}{2}\rho\Delta s_0\left(A_{0f} + M_{0s}\right) + \tfrac{1}{2}\rho\Delta C\left[A_{0f}\left(1 - \ln\left(\tfrac{A_{0f}}{T_0}\right)\right) + M_{0s}\left(1 - \ln\left(\tfrac{M_0 s}{T_0}\right)\right) + T_0\right]$$

$$n_1 = 0.21, n_2 = 0.25, n_3 = 0.11, n_4 = 0.13$$

The implementation of the constitutive model follows the same procedure described in Qidwai and Lagoudas (2000). Basically, given an increment of strain, the incremental form of the SMA constitutive model provides an increment of stress and temperature as an output. The increment of stress and temperature are calculated by implementing the Return Mapping Algorithm. The main difference from this work to Qidwai and Lagoudas (2000) is that the heat equation also needs to be integrated for every increment of stress, whenever the phase transformation is taking place.

The return mapping algorithm solves the thermoelastic-transformation problem defined by the total strain relation, the flow rule, and the thermodynamic driving force π , by dividing it into two problems using an additive split (Qidwai and Lagoudas, 2000). At first, a thermoelastic prediction problem assuming that the increment of the transformation strain is zero is tried. If the predicted thermoelastic state violates the consistency condition, in other words, if it lies outside the transformation surface ($\Phi > 0$), a transformation correction problem takes place to restore the consistency condition. This work uses the Cutting Plane Return Mapping Algorithm as the corrector algorithm. The main idea of the Cutting Plane algorithm is that it relies on integrating the transformation correction equations in an explicit manner

and on linearizing the consistency condition (Qidwai and Lagoudas, 2000). The Newton's iteration method is applied to calculate the increment of martensitic volume fraction. It is important to mention that both return mapping algorithms utilize the same thermoelastic prediction step.

3. NUMERICAL SIMULATIONS

This section presents the numerical simulations of the 1-DOF pseudoelastic oscillator. The cases of forced vibration are going to be presented, for non-isothermal heat convection conditions. Later, the isothermal results, previously published in Machado *et al.* (2007), will be revisited and compared with the non-isothermal case.

3.1 Forced Vibrations - Non-Isothermal Conditions

The case of forced vibration is now considered, where the SMA oscillator 1 is subjected to a sinusoidal excitation. For a given fixed amplitude of the exciting force of $F_0 = 45$N, two single frequency excitation cases will be considered for different excitation frequencies, namely, $f = 15$Hz and $f = 16.7$Hz. The heat transfer coefficient was assumed to be $h = -2.25 \cdot 10^5 \mathrm{W/m^3K}$, while the temperature of the surrounding environment was chosen to be $T_\infty = 293$K.

Figure 2 shows the dynamic response of the oscillator during steady state, for the case of $F_0 = 45$N and $f = 15.0$Hz. Figure 2a shows the stress *vs.* strain curve, while Fig. 2b presents the phase space curve. Figure 2c presents the Poincaré map and the time histories of the Lyapunov exponents are presented in Fig. 2d. It can be notice that the Poincaré map of Fig. 2c presents a cloud of points, that in principle, could be related to the chaotic motion. However, the analyze of the Lyapunov exponents spectrum shows that converged values for this simulation are $(\lambda_1, \lambda_2) = (-3.38, -4.95)$. Since both exponents are negative, the motion of the oscillator for this simulation cannot be classified as a chaotic motion, but in this case, periodic.

Figure 2e presents the temperature variation of the SMA element for this simulation, after it has reached its steady state.

Next, we analyze the oscillator's motion when the excitation frequency is of $f = 21$ Hz, still for the non-isothermal case. Figure 3a presents stress *vs.* strain curve, while Fig. 3b shows the phase-space curve. Figure 3c shows Poincaré section, and the time history of the Lyapunov exponents are presented in Fig. 3d. It can be noticed that the Poincaré map presented in 3c appear as a periodic motion of Period-11, since there are apparently 11 points in the Poincaré map. This periodic motion is confirmed by the analysis of the converged values of the Lyapunov exponents, where both of them present negative values $(\lambda_1, \lambda_2) = (-0.21, -2.63)$. Figure 3e presents the temperature variation of the SMA element due to the thermomechanical coupling.

3.2 Forced Vibration - Isothermal Conditions

The forthcoming analyzes is related to the isothermal oscillations. For the purpose of comparison with the non-isothermal cases, the results presented in Machado *et al.* (2007) for the simulation of an equivalent 1-DOF pseudoelastic oscillator will be revisited.

Figure 4 shows the dynamic response of the oscillator during steady state, for the case of $F_0 = 45$N and $f = 15.0$Hz. Figure 4a shows the stress *vs.* strain curve. Phase space curves, Poincaré map and the time series of the Lyapunov exponents are presented in Fig. 4b, Fig. 4c, and Fig. 4d respectively. Figure 4e shows the temperature variation of the SMA element during the oscillator vibration. This time, instead of a cloud of points as was observed in the case of $f = 15.0$Hz for the non-isothermal case, the Poincaré map of Fig. 4c presents three points, that are related to a period-3 motion. This periodic motion is then confirmed by the analyzes of the spectrum of the Lyapunov exponents, that shows the converged values for this simulation as being $(\lambda_1, \lambda_2) = (-4.74, -4.72)$.

Next, we analyze the oscillator's motion when the excitation frequency is of $f = 21.0$ Hz. Figure 5a presents stress *vs.* strain curve, while Fig. 5b shows the phase space curves and while Fig. 5c the Poincaré map. Figure 5d presents the time history of the Lyapunov exponents, while Fig. 5e shows the temperature change of the SMA element during the simulation. This time, the Poincaré map presents a cloud of points (strange attractor) that can be confirmed to be of a chaotic type by the analyzes of the converged values of the Lyapunov exponents. For this simulation there is of a positive exponent in the spectrum of the Lyapunov exponents $(\lambda_1, \lambda_2) = (3.01, -6.34)$, indicating chaotic response.

4. CONCLUSIONS

This article discussed the nonlinear dynamics and chaos in a pseudoelastic single degree of freedom oscillator. The restitution force was provided by a SMA element described by a constitutive model built upon the Boyd-Lagoudas model, that simulates smooth transitions between the elastic and transformation regimes. Numerical simulations have shown a complex behavior of the oscillator, due to evolving thermomechanical properties and hysteresis. The case of non-isothermal heat convection oscillations was investigated for two different excitation frequencies, and later compared to the isothermal case. As one of the tools to analyze the dynamic response of the oscillator, Lyapunov exponents were

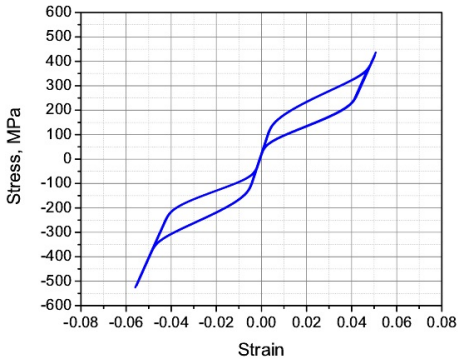

(a) Stress *vs.* Strain

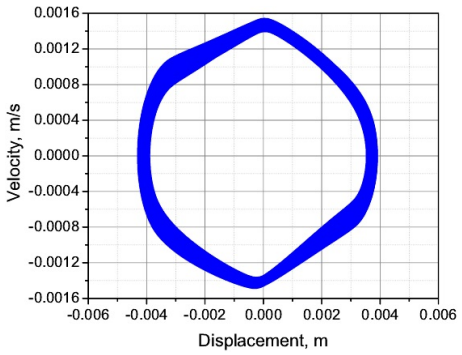

(b) Phase Space Plot

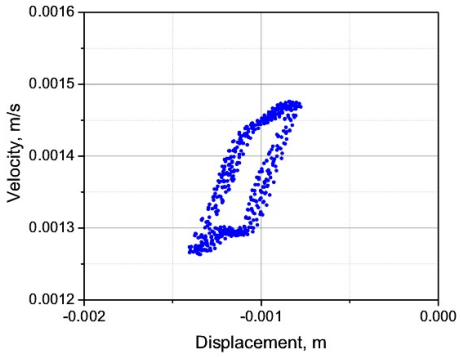

(c) Poincaré Map

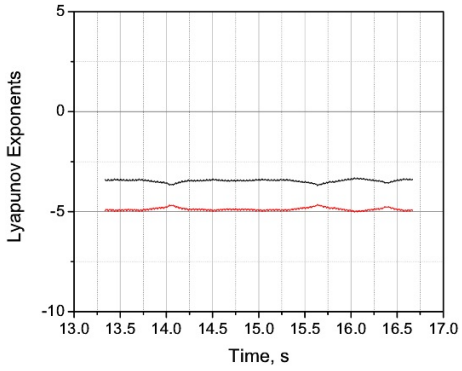

(d) Lyapunov Exponents

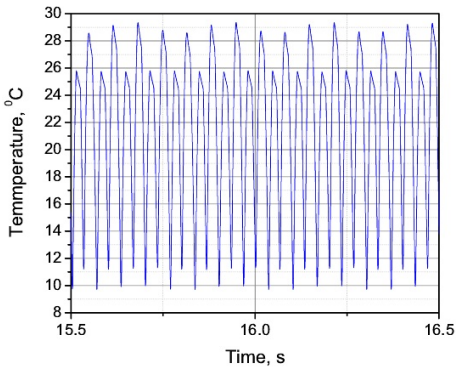

(e) Temperature

Figure 2. Forced response of the SMA oscillator for $F_0 = 45N$ and $f = 15.0$Hz

estimated, by employing the classical algorithm proposed by Wolf *et al.* (1985) using a proper system linearization. The Lyapunov exponents confirmed the presence of chaotic motion of the oscillator for certain excitation frequency values.

5. ACKNOWLEDGMENTS

The authors would like to acknowledge NSF, AFOSR, CAPES (Brazil), and CNPq (Brazil), for the financial support.

6. REFERENCES

Bernardini, D. and Rega, G., 2005, "Thermomechanical Modelling, Nonlinear Dynamic and Chaos in Shape Memory Oscillators", Mathematical and Computer Modelling of Dynamical Systems, Vol.11, No.3, pp.291-315.

Boyd, J. and Lagoudas, D. C.,1996, "A thermodynamical constitutive model for shape memory materials. Part I: the monolithic shape memory alloy", International Journal of Plasticity, Vol.12, No. 6, pp.843-873.

Coleman, B. and Gurtin, M., "Thermodynamics with internal variables", The Journal of Chemical Physics, Vol.47,No.2,pp.597-613.

Feng, Z. C. and Li, D. Z.,1996, "Dynamics of a mechanical system with a shape memory alloy bar", International Journal of Intelligent Material Systems and Structure, Vol.7, pp.399-410.

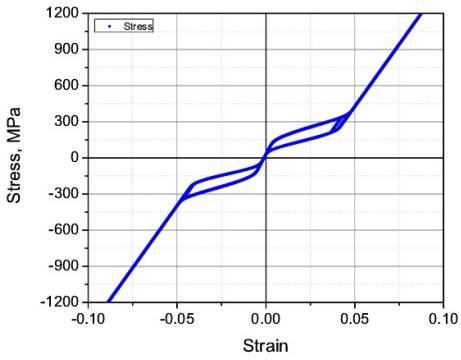

(a) Stress *vs.* Strain

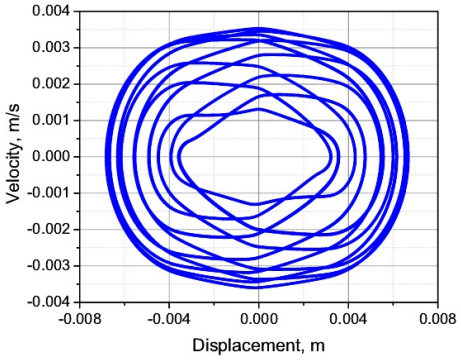

(b) Phase Space Plot

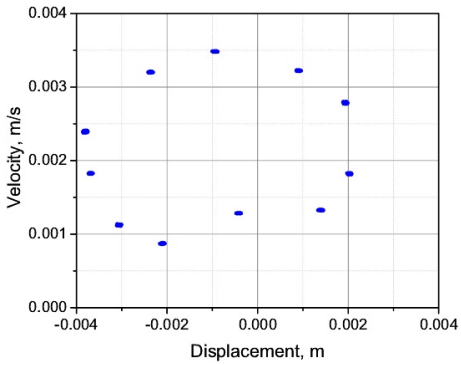

(c) Poincaré Map

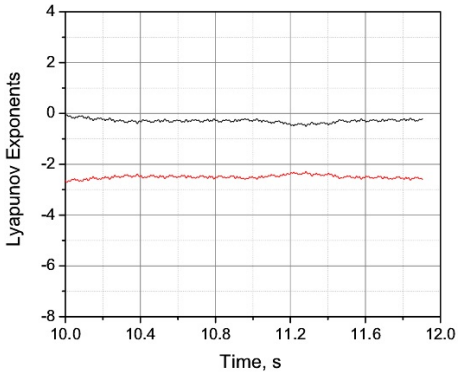

(d) Lyapunov Exponents

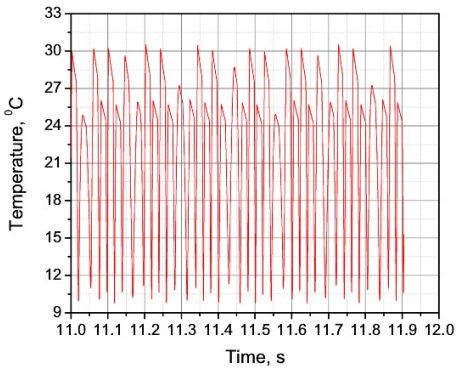

(e) Temperature

Figure 3. Forced response of the SMA oscillator for $F_0 = 45N$ and $f = 21.0$Hz

Lacarbonara, W. and Vestroni, F., 2003, "Nonclassical Response Oscillators with Hysteresis", Nonlinear Dynamics, Vol.32, pp.235-258.

Lagoudas, D. C. and Khan, M. M. and Mayes, J. J. and Henderson, B. K., 2004, "Pseudoelastic SMA Spring Elements for Passive Vibration Isolation. Part II: Simulations and Experimental Correlation", Vol.15, pp.443-470.

Lagoudas, D. C., Machado, L. G. and Lagoudas, M., 2005, "Nonlinear Vibration of a One-Degree of Freedom Shape Memory Alloy Oscillator: A Numerical-Experimental Investigation", in 46th AIAA/ ASME / ASCE / AHS / ASC Structures, Structural Dynamics and Materials Conference, pp.1-18, April 18-21, Austin, TX. USA.

Leo, P. H., Shield, T. W. and Bruno, O. P.,1993, "Transient Heat Transfer Effects on the Pseudoelastic Behavior of Shape-Memory Wires", Acta Metallurgica and Materialia, Vol.41, No.8, pp.2477-2485.

Machado, L. G. and Lagoudas, D. C., 2004, "Dynamical Response of Shape Memory Alloys", in 2004 ASME International Mechanical Engineering Congress, (Anaheim, CA. USA), November, 13-19.

Machado, L. G. and Lagoudas, D. C., 2006, "Nonlinear Dynamics of a SMA Passive Vibration Damping Device",in Smart Structures and Materials 2006: Damping and Isolation, SPIE, pp.6169X.

Machado, L. G., Savi, M. A. and Pacheco, P. M. C. L., 2003, "Nonlinear Dynamics and Chaos in Coupled Shape Memory Oscillators", International Journal of Solids and Structures, Vol.40, pp.5139-5156.

Machado, L. G., Lagoudas, D. C. and Savi, M. A., 2007, "Nonlinear Dynamics and Chaos in a Shape Memory Alloy

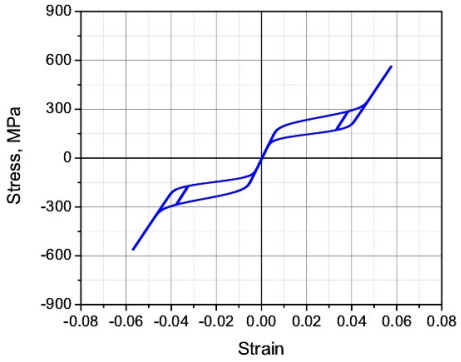

(a) Stress *vs.* Strain

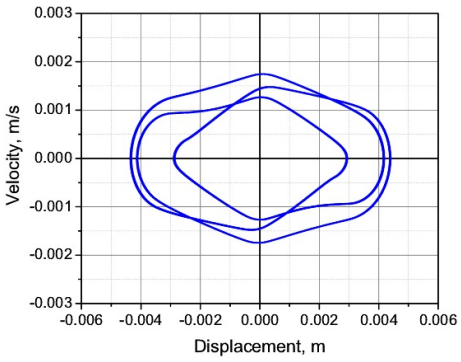

(b) Phase Space Plot

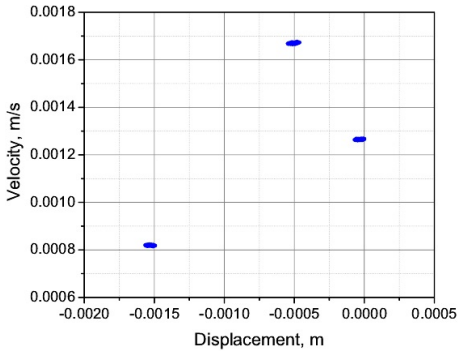

(c) Poincaré Map

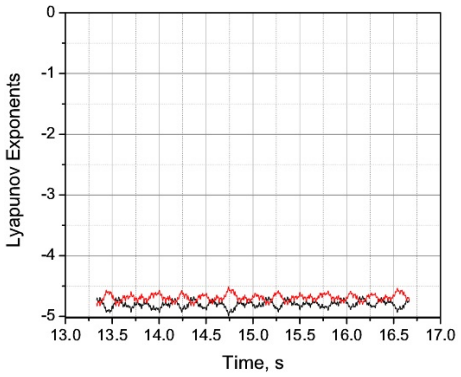

(d) Lyapunov Exponents

Figure 4. Forced response of the SMA oscillator for $F_0 = 45N$ and $f = 15.0$Hz

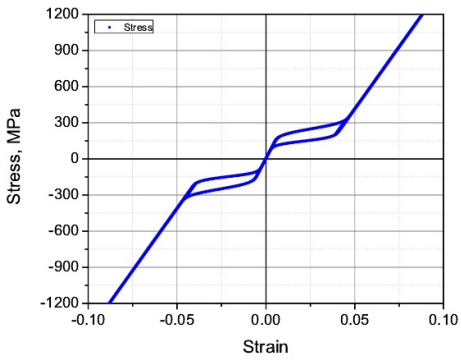

(a) Stress *vs.* Strain

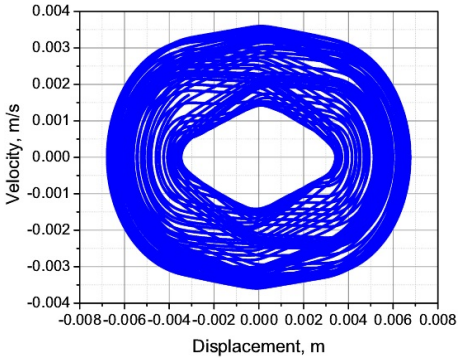

(b) Phase Space Plot

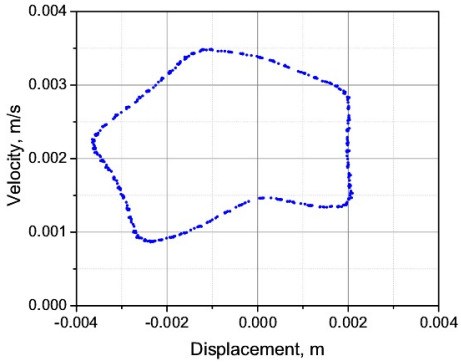

(c) Poincaré Map

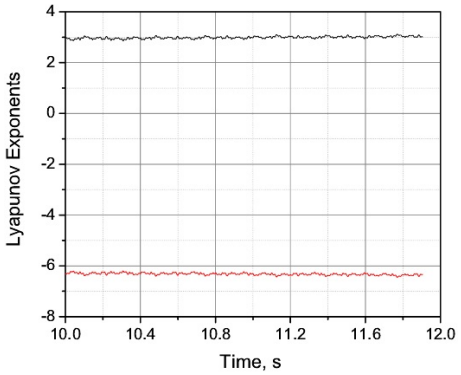

(d) Lyapunov Exponents

Figure 5. Forced response of the SMA oscillator for $F_0 = 45N$ and $f = 21.0$Hz

Pseudoelastic Oscillator", in Smart Structures and Materials 2007: Actuators and Damping, SPIE.

Oberaigner, E. R., Fisher, F. D. and Tanaka, K.,2002, "On the optimal damping of a vibrating shape memory alloy rod", Journal of Engineering Materials and Technology, Vol.124, pp.97-102.

Qidwai, M. A. and Lagoudas,D. C., 2000, "Numerical Implementation of a Shape Memory Alloy Thermomechanical Constitutive Model Using Return Mapping Algorithm", International Journal for Numerical Methods in Engineering, Vol.47, pp.1123-1168.

Salich, Z., Hou, J. and Noori, M.,2001, "Vibration Supression of Structures Using Passive Shape Memory Alloy Energy Dissipation Devices", Journal of Intelligent Material Systems and Structures, Vol.12, No. 10, pp.671-680.

Saadat, S., Salich, J., Noori, M., Hou, Z., Davoodi, H., Bar-on, I., Suzuki, Y., and Masuda, A., "An Overview of Vibration and Seismic Applications of NiTi Shape Memory Alloy",Smart Materials and Structures, Vol.11, pp. 218-229.

Savi, M. A. and Pacheco, P. M. C. L., 2002, "Chaos and Hyperchaos in Shape Memory Systems", International Journal of Bifurcations and Chaos, Vol.12, No.3, pp.645-657.

Savi, M. A. and Sa, M. A. N. and Pacheco, P. M. C. L., 2006, "Tensile-Compressive Asymmetry Influence on Shape Memory Alloy Systems", Chaos, Solitons and Fractals, Vol. xx, No. XX, 2006.

Shaw, J. A. and Kyriakides, S., 1995, "Thermomechanical Aspects of NiTi", Journal of Mechanics and Physics of Solids, Vol.48, No.8, pp.1243-1281.

Williams, K., Chiu, G. and Bernhard, R.,2002, "Adaptive-Passive Absorbers Using Shape-Memory Alloys", Journal of Sound and Vibration, Vol.249, No.5, pp.835-848.

Wolf, A., Swift, J. B., Swinney, H. L. and Vastano, J. A., 1985, "Determining Lyapunov Exponents From a Times Series", Physica D, Vol.16, pp.285-317.